Chemistry & Biology, Vol. 11, 1269–1277, September, 2004, ©2004 Elsevier Ltd. All rights reserved. DOI 10.1016/j.chembiol.2004.07.014

Amphidinolide H, a Potent Cytotoxic Macrolide, Covalently Binds on Actin Subdomain 4 and Stabilizes Actin Filament

Takeo Usui,[1] Sayaka Kazami,[1] Naoshi Dohmae,[2] Yoshikazu Mashimo,[3] Hisae Kondo,[1] Masashi Tsuda,[5] Asako Goi Terasaki,[4] Kazuyo Ohashi,[3] Jun'ichi Kobayashi,[5] and Hiroyuki Osada[1,*]

[1]Antibiotics Laboratory and
[2]Biomolecular Characterization Team
RIKEN Discovery Research Institute
2-1 Hirosawa, Wako-shi, Saitama 351-0198
Japan
[3]Department of Biology
Faculty of Science
Chiba University
[4]Graduate School of Science and Technology
Chiba University
Yayoicho, Inage-ku, Chiba 263-8522
Japan
[5]Graduate School of Pharmaceutical Sciences
Hokkaido University
Sapporo 060-0812
Japan

Summary

The actin-targeting toxins have not only proven to be invaluable tools in studies of actin cytoskeleton structure and function but they also served as a foundation for a new class of anticancer drugs. Here, we describe that amphidinolide H (AmpH) targets actin cytoskeleton. AmpH induced multinucleated cells by disrupting actin organization in the cells, and the hyperpolymerization of purified actin into filaments of apparently normal morphology in vitro. AmpH covalently binds on actin, and the AmpH binding site is determined as Tyr200 of actin subdomain 4 by mass spectrometry and halo assay using the yeast harboring site-directed mutagenized actins. Time-lapse analyses showed that AmpH stimulated the formation of small actin-patches, followed by F-actin rearrangement into aggregates via the retraction of actin fibers. These results indicate that AmpH is a novel actin inhibitor that covalently binds on actin.

Introduction

Anticancer drug development strategies have traditionally focused on direct inhibition of cancer cell growth. However, other rate-limiting processes in the progression of cancers are also promising targets for intervention. Tumor cell invasion and metastasis, later points in cancer progression, are inherently thought to be involved in cell motility [1, 2]. Therapeutic agents that potently inhibit invasion and metastasis could be effective in restraining new tumor formation when earlier therapy or surgery has failed, or could increase successful containment of solid tumors in combination therapy with other agents. Therefore, proteins involved in cell motility represent attractive targets for development of new chemotherapies [3]. Dynamic processes such as cell migration and division depend on the actin cytoskeleton, a dense meshwork of protein polymers capable of undergoing rapid cycles of assembly and disassembly, under the control of a large number of actin-associated proteins. It is known that the actin cytoskeleton is substantially modified in transformed cells, and this occurs in concert with changes in a host of actin filament-associated regulatory proteins. These changes are thought be integrally involved in the abnormal growth properties of tumor cells, their ability to adhere to tissue, and their increased ability to metastasize. Therefore, small molecules that act on the actin cytoskeleton of tumor cells and thus inhibit cell division and movement may be of high therapeutic value.

Several actin inhibitors are reported, and these compounds are largely classified into two types: destabilizer and stabilizer of actin filaments. Cytochalasins and latrunculins are the most famous actin filament destabilizers and are widely used for analyses of cellular functions of actin [4–7]. Mycalolide B [8, 9], swinholide A [10, 11], aplyronine A [12, 13], and misakinolide A [14, 15] destroy the actin cytoskeleton by severing and/or sequestering actin. The other class of compounds, actin stabilizers, also has been reported. Phalloidin, a mushroom toxin, stabilize F-actin by binding at the junction of two or three actin monomers in the filament and has been widely utilized for analysis of actin dynamics [16, 17]. Jasplakinolide, a cyclodepsipeptide, binds F-actin competitively with phalloidin and induces polymerization of monomeric actin as well as stabilizes actin filaments [18, 19]. Other stimulators of actin assembly have been reported [20–23], and some of these compounds are under investigating for clinical trials.

It is important to determine the binding site of these drugs to their target proteins for understanding the inhibition mechanism and development of specific inhibitors. Latrunculin A binds in the interface between subdomains 2 and 4, and clamps the ATP binding site, suggesting that latrunculin A inhibits actin polymerization via inhibiting the nucleotide exchange [24]. Recently, two epoch-making studies on actin binding drugs were reported. Klenchin et al. reported that kabiramide C and jaspisamide A, two actin polymerization inhibitors, bound a site almost identical to that bound by gelsolin domain 1 [25]. Based on these results and the biochemical data of Tanaka et al. [26], Klenchin et al. speculated that both compounds mimic the binding of gelsolin family proteins. Oda et al. also reported that dolastatin 11, an F-actin stabilizer, binds in the gap between the two long-pitch F-actin strands, and speculated that the connection between the strands might be a key for the F-actin stabilization [27]. These studies clearly showed that the investigation of the drug binding site is informative for elucidating the inhibitory mechanism.

*Correspondence: osadah@riken.jp

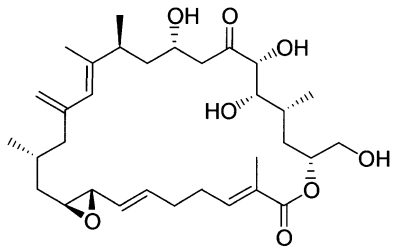

Figure 1. Structure of AmpH

Amphidinolides are a series of unique cytotoxic macrolides isolated from dinoflagellates *Amphidinium* sp., which were separated from marine acoel flatworms *Amphiscolops* sp. [28]. Amphidinolide H (AmpH) is a potent cytotoxic 26-membered macrolide possessing unique structural features such as an allyl epoxide and vicinally located one-carbon branches (Figure 1) [29]. The absolute stereochemistry of AmpH has been established on the basis of the X-ray diffraction analysis and synthesis of a degradation product [30]. From the structure-activity relationship of AmpH-type macrolides, it was found that the presence of an allyl epoxide, an *S-cis*-diene moiety, and the ketone at C-20 was important for the cytotoxicity [31]. Although AmpH shows a potent cytotoxicity to several carcinoma cell lines at the picogram level, the target molecule is unclear. Here, we describe that the target molecule of AmpH is actin cytoskeleton. AmpH is the first compound that binds actin polymer covalently and its binding site is located on the actin subdomain 4.

Results

Effects of AmpH on the Mammalian Cells

AmpH shows a potent cytotoxicity against murine lymphoma L1210 and human epidermoid carcinoma KB cells with picogram order IC_{50} values [29]. To clarify the effects of AmpH on the cells, we investigated the effect of AmpH on the cell cycle in exponentially growing rat normal fibroblast 3Y1 cells. The distribution profile of cellular DNA contents after 42 hr of 100 nM AmpH treatment was determined by flow cytometry (Figure 2A). Four peaks corresponding to 2C, 4C, 8C, and 16C were observed in AmpH-treated cells (+AmpH; Figure 2A), meaning AmpH induced polyploid cells. By phase contrast observation, AmpH-induced polyploid cells were larger than nontreated cells, and most of the AmpH-treated cells possessed two or more nuclei (Figures 2B and 2C). It is known that these phenotypes occur by cytokinesis inhibition, such as that by treatment with cytochalasin B, an actin polymerization inhibitor [32]. To determine whether or not AmpH interferes with the functions of the actin cytoskeleton, we observed the cytoplasmic actin stress fibers by fluorescence microscopy (Figures 2D–2I). In the control cells, we observed actin stress fibers running from one edge of the cell to the other (Figure 2D). After 6 hr of treatment with 30 nM AmpH, the actin stress fibers had completely disappeared, and only a few disorganized aggregates remained in the cells (Figure 2G), but the microtubule networks were not affected (Figure 2H). The actin morphology of AmpH-treated cells resembled that of cells treated with a potent actin polymerization stimulator, jasplakinolide [18] (Figure 2J). The effect of AmpH was also irreversible, at least in a day (data not shown).

AmpH Stimulates Actin Polymerization and Stabilizes F-Actin In Vitro

The phenotype of the cell treated with AmpH resembled that with jasplakinolide, actin stabilizer [18, 19]. To evaluate that AmpH is an F-actin inducer, we examined actin polymerization by the standard fluorescence assay (copolymerization of actin and pyrenyl-labeled actin). K^+-actin started polymerization after the apparent lag time (Figure 3A, open squares). In the presence of jasplakinolide, actin polymerization started immediately without no apparent lag time (Figure 3A, open circles). This result is consisted with previous report that jasplakinolide stimulated nucleation step [19]. On the other hand, there is an apparent lag time in the presence of AmpH; however, net fluorescent intensity increased with dose dependently (Figure 3A, closed symbols). Although the effective concentrations of both AmpH and jasplakinolide were almost same in situ, higher concentrations of AmpH were required to promote actin polymerization in vitro. The same results were obtained in the case of pyrenyl-labeled Mg^{2+}-actin (data not shown). We next examined the effects of AmpH on depolymerization of Mg^{2+}-F-actin (Figure 3B). Depolymerization started immediately after 1/10 dilution of pyrenyl-labeled Mg^{2+}-F-actin into buffer G. AmpH prevented depolymerization of F-actin in a dose-dependent manner. The time required to achieve stabilization of F-actin was less than or equal to the time required to mix the sample (5 s). These results clearly showed that AmpH promotes actin polymerization and stabilizes F-actin.

To confirm that the increase in fluorescence intensity reflected actin polymerization, samples were negatively stained with uranyl acetate and examined by electron microscopy (Figure 3C). Numerous 9 nm wide filaments were present in the samples with AmpH, and their appearance was indistinguishable from that of control.

AmpH Covalently Binds Actin In Vitro and In Situ

It is known that some bioactive compounds containing epoxide bind their target molecules covalently [33–36]. Since the structure-activity relationships showed that an allyl epoxide is important for the cytotoxicity of AmpH [31], there is a possibility that AmpH covalently modifies actin via epoxide. To clarify this possibility, we investigated the change of molecular weight of actin after AmpH treatment by MALDI-TOF mass spectrometry (Figure 4A). The molecular weight of native actin was determined to be 41,988 (−AmpH; Figure 4A), but that of AmpH-treated actin was 42,524 (+AmpH; Figure 4A). The difference, 536, was thought to represent the molecular weight of AmpH (562). This binding is highly specific, because treatment with a 10× excess molar amount of AmpH resulted in the mass increase corresponding to only one AmpH. To determine the AmpH binding site on actin, native and AmpH-treated actin were alkylated and digested with trypsin, and the generated peptides

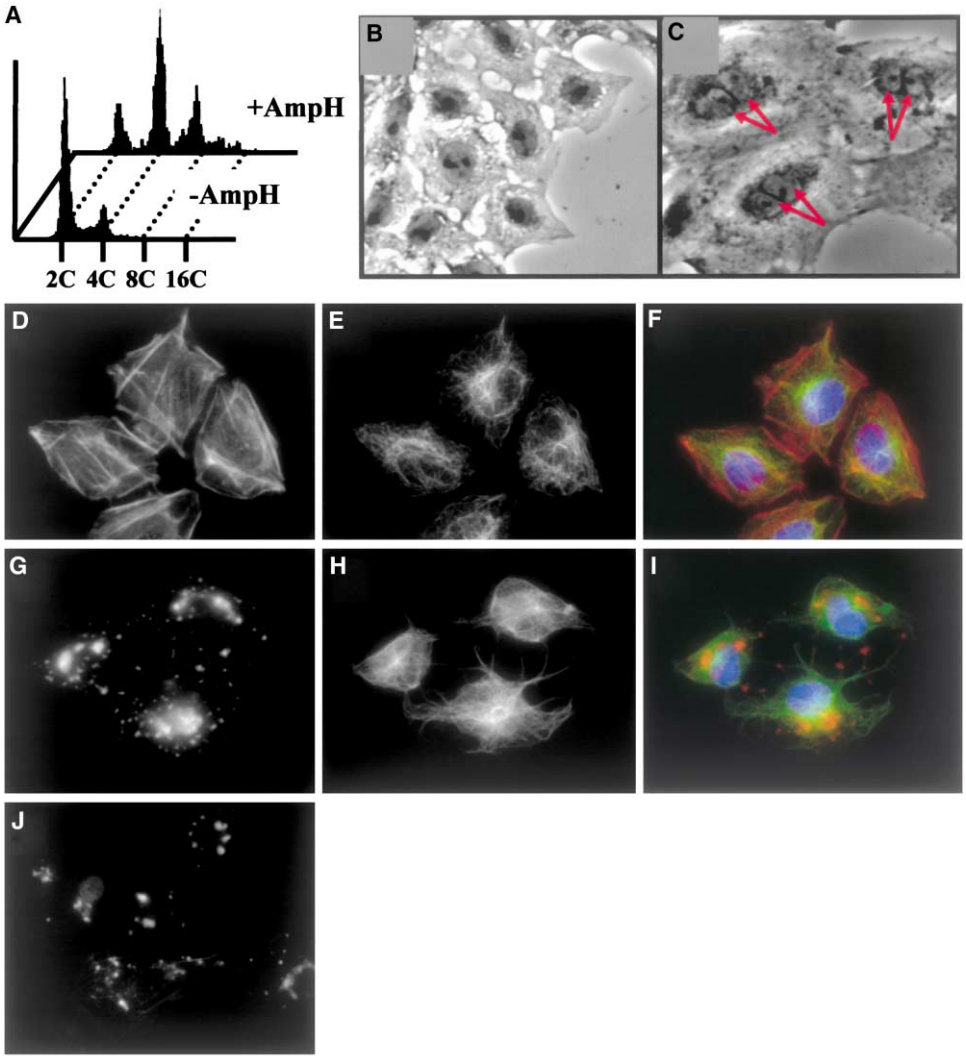

Figure 2. Effects of AmpH on 3Y1 Cells

(A) Effects of AmpH on the distribution of DNA content in asynchronous 3Y1 cell culture was analyzed by flow cytometry. Asynchronous 3Y1 cells were treated with 300 nM AmpH for 0 (−AmpH) or 42 hr (+AmpH).

(B and C) Binucleated cell formation by AmpH. 3Y1 cells were treated with 300 nM AmpH for 0 (B) or 42 hr (C). Binucleated cells were indicated by red arrows.

(D–I) Effects of AmpH on the actin and tubulin cytoskeletons. 3Y1 cells were treated with 30 nM AmpH for 0 (D–F) or 6 hr (G–I). (D and G) Actin cytoskeleton stained with rhodamine-phalloidin. (E and H) Tubulin cytoskeletons stained with anti-β-tubulin antibody. (F and I) Merged images with actin (red), tubulin (green), and DNA (blue, stained with Hoechst 33258) are shown.

(J) Effect of jasplakinolide on the actin cytoskeleton. 3Y1 cells were treated with 30 nM jasplakinolide for 6 hr.

were analyzed with MALDI-TOF/TOF mass spectrometry. The amino acid sequences of the digested peptides were deduced based on the molecular masses. The mass corresponding to peptide Gly_{199}-Arg_{208} (1130.5 mass) had disappeared, and a single extra mass, 1692.8, appeared in AmpH-treated protein (Figure 4B). This new fragment mass corresponded to the AmpH-adduct of peptide Gly_{199}-Arg_{208}. These results clearly show that AmpH covalently binds to the Gly_{199}-Arg_{208} fragment of actin. Although we performed a detailed MS/MS analysis to identify the exact binding site of AmpH, we obtained the original peptide mass without AmpH binding as a main peak. This result suggests that the bond between AmpH and peptide is readily broken under the MS/MS condition.

Amphidinolide H Covalently Binds on Tyr200

If the interaction between the drug and its cellular target is impaired by mutation, this would lead to a dominant phenotype specifically resistant to the drug. Because actin is a highly conserved protein and AmpH inhibited the growth of the wild-type yeast strain by inhibiting the function of actin (data not shown), we next tested the AmpH sensitivity of the yeast cells carrying an actin mutant. Since allyl epoxide is reactive with hydroxyl moiety, there are five candidate residues for the AmpH binding residue on *ACT1*: Tyr198, Ser199, Ser201, Thr202, and Thr203. Cells from which the chromosomal *ACT1* was deleted and which were kept alive by *ACT1* on a *URA3*-based plasmid were transformed with *LEU2*-based plasmids containing site-directed mutagenized

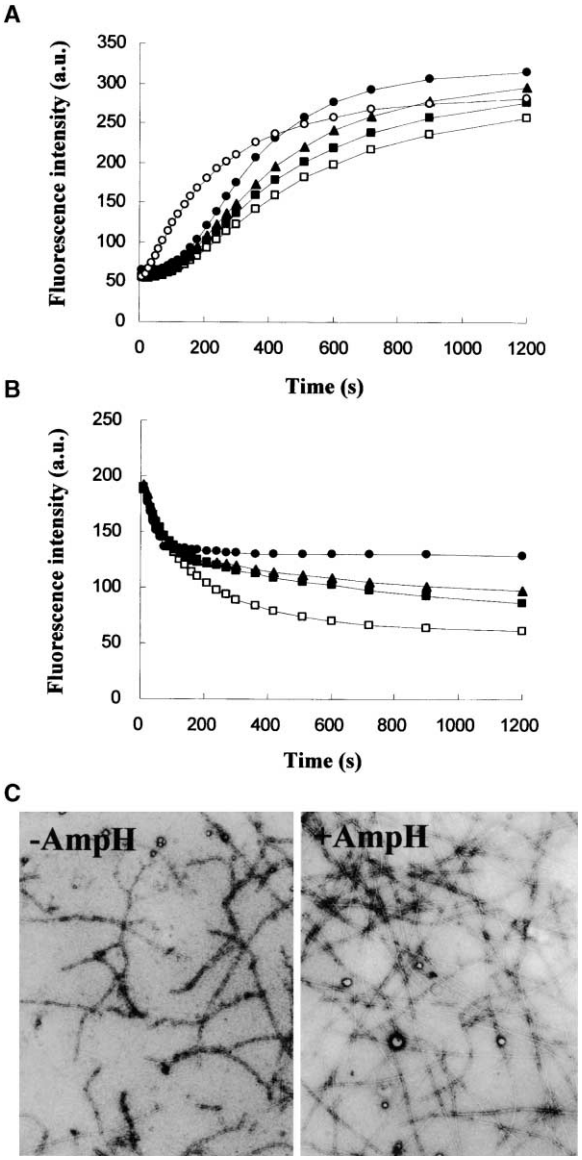

Figure 3. Effects of AmpH on Actin Polymerization In Vitro

(A) Effects of AmpH on the copolymerization of actin and pyrenyl-labeled actin. Actin/pyrenyl-labeled actin (4 μM) was incubated with jasplakinolide (open circle, 300 nM), AmpH (closed squares, 10 μM; closed triangles, 20 μM; closed circles 50 μM), or without chemicals (open squares). Polymerization was started by the addition of inducing salts (100 mM KCl, 1 mM $MgCl_2$, 1 mM ATP) and drugs solved in DMSO at time 0 (final 1% DMSO in reaction mixture).

(B) Effects of AmpH on the depolymerization of actin and pyrenyl-labeled actin. Pyrenyl-labeled actin Mg^{2+}-F-actin (4 μM) was diluted to 0.4 μM. After 75 s, AmpH was added. The samples were mixed to give final concentrations of 10 μM (closed squares), 50 μM (closed triangles), 100 μM (closed circles), or 0 μM (open squares) AmpH.

(C) Electron microscopy of actin polymer formed in the presence or absence of AmpH. 24,000×.

ACT1. Cells were then tested for growth on 5-fluoroorotic acid (5-FOA). Because the 5-FOA selects against the *URA3*-based *ACT1* plasmid, the *LEU2*-based *ACT1* construct was the only source of *ACT1* activity in the 5-FOA-resistant colonies. All *ACT1* mutants complemented Δ*act1*, suggesting that these *ACT1* mutants function in yeast (Figure 5A). The obtained *ACT1* mutant cells were subjected to a halo assay [37]. Because cells carrying the wild-type and all of the cells containing the *ACT1* mutants showed growth inhibition against latrunculin A, we concluded that these mutations were not responsible for latrunculin A resistance (data not shown). Although cells carrying the wild-type and *ACT1* mutants, with the exception of the Tyr198Phe *ACT1* mutant, were sensitive to AmpH, Tyr198Phe *ACT1* mutant cells showed AmpH resistance (Y198F; Figure 5B). This result strongly suggests that Tyr198 (corresponding to Tyr200 on mammalian actin) on actin is involved in the AmpH binding.

F-Actin Aggregation Formed by Retraction of Preexisted Stress Fiber

It is known that jasplakinolide, which stimulates actin polymerization, causes the accumulation of F-actin aggregates in cells, as observed in Figure 2J [38]. Bubb et al. proposed that this phenomenon is caused by formation of multiple actin filament nuclei with fiber propagation limited by the resulting shortage of monomeric actin in the cells [19]. To examine this model, we investigated the process of the formation of F-actin aggregates in detail by time-lapse video microscopy with 5 s intervals using GFP-β-actin-expressing cells. Before AmpH addition, the dynamic movements of lamellipodia were observed (Figure 6A, arrow). Within 30 s after addition of 250 nM AmpH, the movements of lamellipodia had completely ceased (Figure 6A, arrow), and several small actin clumps had emerged in the cell (Figures 6A and 6B). Within 10 min after the addition of AmpH, drastic morphological changes occurred by the retraction of actin stress fibers, and large actin aggregates were formed in the cell. These results clearly show that the large F-actin aggregates are derived from preexisting stress fibers.

Discussion

AmpH Is a Novel Actin Stabilizer

Anti-actin compounds have the potential to function as anticancer drugs. In this paper, we report that AmpH, a potent cytotoxic compound, targets and stabilizes actin cytoskeleton. AmpH induced the formation of polyploid cell containing multiple nuclei (Figures 2A–2C). Such a phenotype is typical for that of drugs which interfere with the function of actin cytoskeleton. To elucidate that AmpH interferes with the functions of actin, we observed the distributions of F-actin by staining with rhodamine-phalloidin. Although many actin stress fibers were observed in control fibroblast cells, there were no actin stress fibers in the AmpH-treated cells. Instead, there were many irregular aggregates (Figure 2G). These phenotypes resembled that of jasplakinolide, a stimulator for actin polymerization [19, 39] (Figure 2J). As expected, AmpH stimulated the polymerization of pyrenyl-labeled actin and stabilized preformed F-actin (Figures 3A and 3B). These results clearly showed that AmpH is a novel actin stabilizer.

Are the effects of AmpH on the actin the same with jasplakinolide? Our data, that jasplakinolide stimulated the pyrenyl-labeled actin polymerization with no obvious

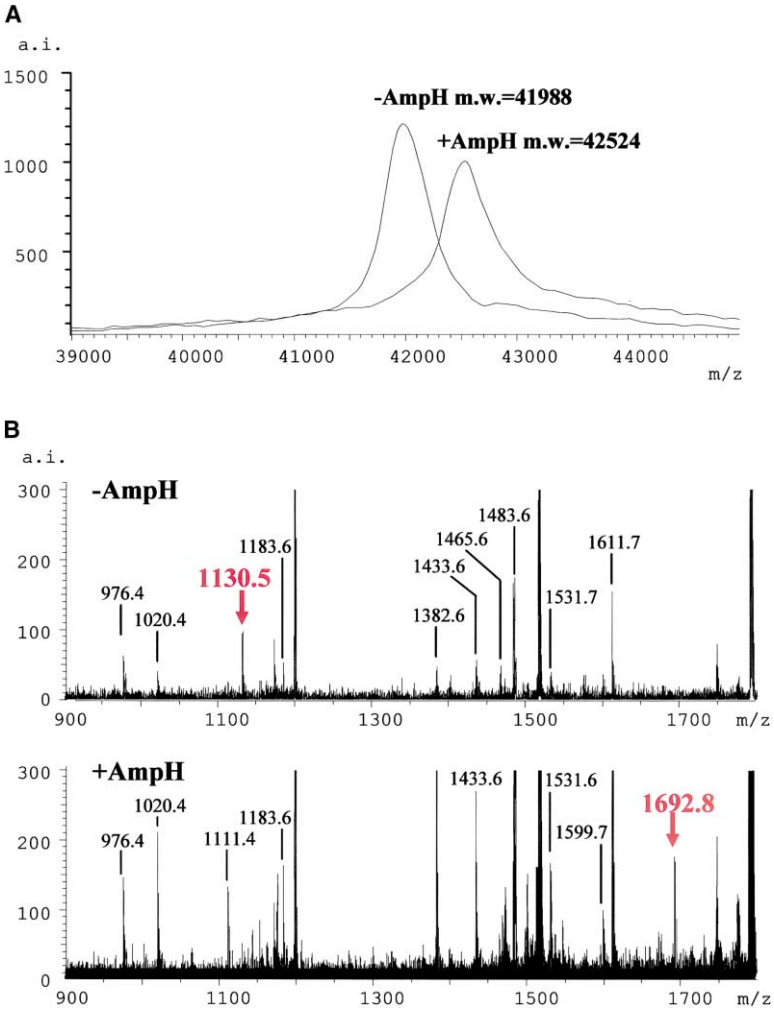

Figure 4. AmpH Covalently Modified Actin In Vitro

(A) MALDI-TOF MS analysis of AmpH-treated actin.

(B) MALDI-TOF/TOF MS analysis of trypsin-digested actin. 1130.5 mass fragment in the upper panel is corresponding to 199–208 aa of α-actin. In the lower panel (amphidinolide H treated), 1130.5 mass fragment was disappeared and 1692.8 mass fragment (corresponding to 199−208 aa of α-actin + AmpH) was observed.

lag time, is consistent with the previous report that jasplakinolide augments nucleation (Figure 3A, [19]). In contrast, there were lag time in the pyrenyl-labeled actin polymerization induced by AmpH, nevertheless the mass of polymerized actin increased. Furthermore, AmpH did not facilitate the nucleation even in the preincubation of G-actin under nonpolymerizing condition (data not shown). These results strongly suggest that the effects of AmpH on actin are different from that of jasplakinolide. Since it is suggested that phalloidin,

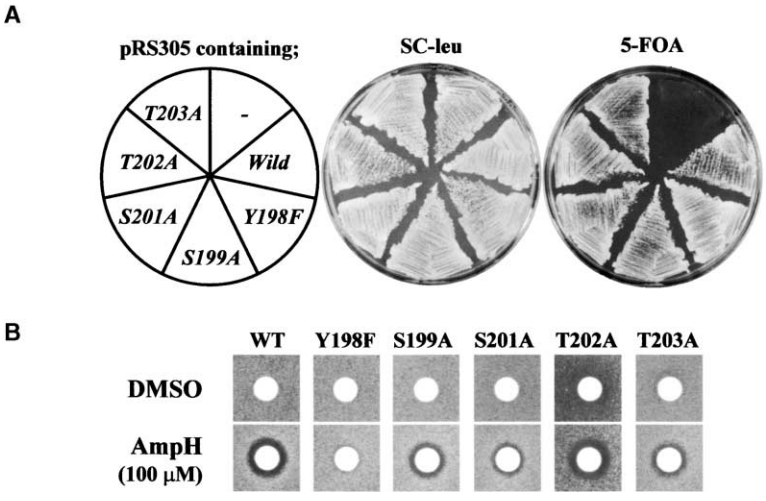

Figure 5. Yeast *act1-Y198F* Showed AmpH Resistance In Situ

(A) Site-directed mutagenized actins support the viability of the cells lacking wild-type actin.

(B) The cell harboring Y198F-mutated actin is resistant against AmpH.

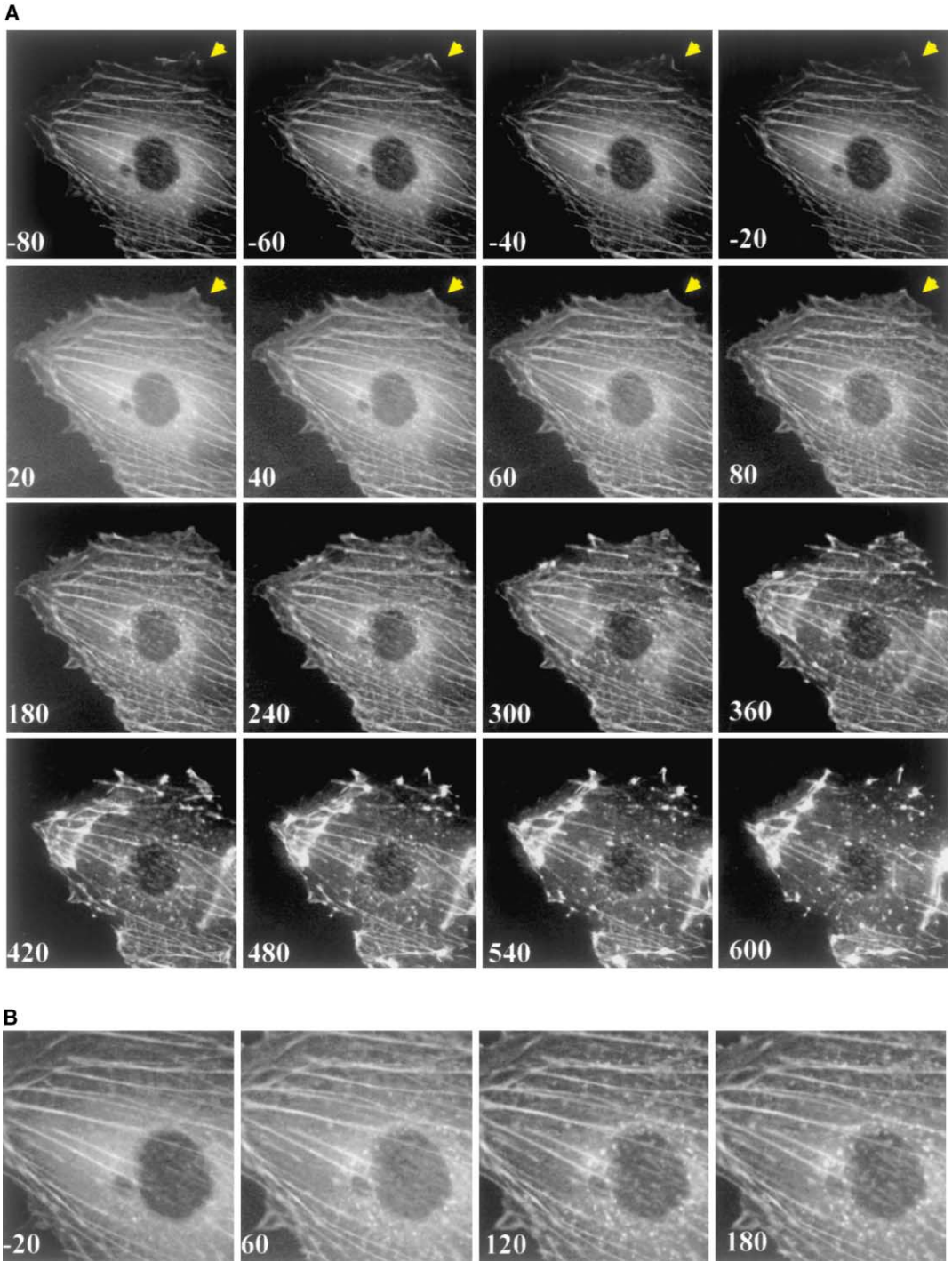

Figure 6. Time-Lapse Analysis of the Actin Cytoskeleton In Situ

(A) 250 nM AmpH was added at time 0, and collection time(s) of the images of GFP-β-actin-expressing 3Y1 cells were shown.
(B) 2× magnification of (A).

without a large effect on the rate constant for nucleation, stabilizes F-actin by decreasing the rate of dissociation of actin oligomer [40], AmpH might be a phalloidin-type compound. To elucidate the actin stabilization mechanism of AmpH, the quantitative evaluation of nucleation and elongation rate constants should be investigated.

AmpH Covalently Binds to Actin

As expected from the analysis of the structure-activity relationships [31], the covalent binding of AmpH to the target protein, actin, was elucidated by MALDI-TOF mass spectrometry (Figure 4A). The binding is specific and only one AmpH binds to one actin protein. The

binding site of AmpH was determined by MALDI-TOF mass spectrometry as the fragment Gly199-Arg208, which participates in a loop in the actin subdomain 4 (Figure 4B). This region is important for regulation of actin dynamics; for example, actin-fragmin kinase phosphorylates at residues Thr203 and Thr202, and abolishes the nucleating activity in *Physarum polycephalum* [41]. Furthermore, the AmpH binding region is close to the actin-actin contact between subdomain 4 of one subunit and subdomain 1 of the diagonally located subunit in the F-actin model refined by Tirion and coworkers [42]. It is widely believed that the diagonal contact is relatively weak in the F-actin structure. Therefore, strengthening the diagonal contact, either directly by binding of the drug or through the conformational change induced by drug binding, should induce F-actin stabilization.

We also determined that the Tyr200 on actin subdomain 4 is key residue for AmpH-covalent binding. Since hydroxyl moiety is not highly reactive nucleophile compared to sulfhydryl moiety, there is a possibility that Tyr200 is in a special environment making it more reactive. Supporting this possibility, AmpH did not bind to the peptide of the AmpH binding subdomain (data not shown). Furthermore, AmpH did not facilitate the nucleation (Figure 3A) but quickly stabilized F-actin (Figure 3B). These results suggest that AmpH binding pocket is formed when actin polymerizes, and that AmpH could not bind to monomeric actin.

F-Actin Aggregation Formed by Retraction of Preexisted Stress Fiber

It is known that the drug, which stimulates actin polymerization, cause the accumulation of F-actin aggregates in the cells as observed in Figures 2G and 2J. Bubb et al. [19] proposed that this phenomenon is caused by formation of multiple actin filament nuclei in the drug-treated cells, with fiber propagation limited by the resulting shortage of monomeric actin in the cells. To examine this model, we investigated the process of the formation of F-actin aggregates in detail by the time-lapse observation using GFP-β-actin-expressing cells. AmpH inhibited the movement of lamellipodia completely and induced the formation of several small actin clumps in a minute (Figure 6). Inhibition of the dynamic movement of lamellipodia indicates that AmpH stabilizes the dense network of actin filaments without either polymerization or depolymerization of actin. The inhibition of actin polymerization might be due to the deprivation of free G-actin via inhibition of the treadmilling of lamellipodia. Small actin clumps might be short actin filaments, and their formation was observed not only in the cells treated with AmpH but also in those treated with jasplakinolide (data not shown). These results would seem to be paradoxical, since the in vitro activity of AmpH is different from that of jasplakinolide (Figure 2A). Unlike jasplakinolide, AmpH shows no apparent nucleation activity in vitro. One possibility is that AmpH exerts its nucleation activity in vivo via regulation of the activity of actin binding proteins, such as the Arp2/3 complex. Alternatively, AmpH only stabilizes short actin filaments, which are formed by spontaneous nucleation. These small clumps did not form large aggregates, suggesting that the supply of free G-actin, required for the aggregate formation, is limited by the same mechanism in lamellipodia.

Within the next 10 min, drastic morphological changes occurred by the retraction of actin stress fibers, and large actin aggregates were formed in the cell. Since the same results were obtained in the case of jasplakinolide (data not shown), this is the common feature of actin-stabilizing drugs. However, these results are not consistent with the previous model [19]. In the previous model, the significant aggregate-formation starts only after the remodeling of stress fibers sufficiently augments the G-actin pool to allow for drug-induced filament nucleation. However, F-actin aggregates were formed by the retraction of preexisting stress fibers in the presence of AmpH and jasplakinolide. These results suggest that the new nucleated filaments might not be required for the formation of F-actin aggregates, although small actin clumps were also formed by drug treatment. Further investigation will be needed to determine how AmpH initiates the retraction of preexisting stress fibers.

Significance

The actin-targeting toxins have not only proven to be invaluable tools in studies of actin cytoskeleton structure and function but they also served as a foundation for a new class of anticancer drugs. In this paper, we found that AmpH, a potent cytotoxic macrolide, targets actin cytoskeleton and stabilizes F-actin. Different from previously reported F-actin stabilizers, AmpH covalently binds on actin. We determined that AmpH binding site is Tyr200 of actin subdomain 4 by mass spectrometry and the systematic mutagensis of yeast actin. This residue is close to the actin-actin contact between subdomain 4 of one subunit and subdomain 1 of the diagonally located subunit in the F-actin. As the other F-actin stabilizers, for example, phalloidin, jasplakinolide, and dolastatin 11, also locate the same actin-actin contact site, strengthening the diagonal contact might be a common feature of F-actin stabilizers. We also showed that AmpH stimulated F-actin rearrangement into aggregates via the retraction of actin fibers. AmpH should be a useful tool to investigate the regulation of actin stress fiber.

Experimental Procedures

Cell Culture, Flow Cytometry, and Immunofluorescence Procedure

3Y1 cells (rat normal fibroblasts) and HT1080 cells (human fibrosarcoma) were cultured in Dulbecco's modified Eagle's medium supplemented with 10% fetal calf serum in a humidified atmosphere containing 5% CO_2. The flow cytometry and immunofluorescence procedures were performed as described previously [43]. GFP-fused β-actin was a gift from Prof. Gerard Marriott (University of Illinois, Champaign-Urbana, IL) and transfected into exponentially growing 3Y1 cells with Effectene Transfection Reagent (Qiagen, Tokyo, Japan), and GFP signals were observed with a DeltaVision system (Applied Precision, Issaquah, WA) including an Olympus IX70 inverted microscope (Olympus, Tokyo, Japan), with a 60× (numerical aperture, 1.4) objective lens and an Olympus MI-IBC stage-heating device (Olympus). Images were captured with a cooled, charge-coupled-device camera from Princeton Instruments (Trenton, NJ). 180–360 optical images were captured at 5 s intervals,

and out-of-focus light was removed by iterative deconvolution on a Silicon Graphics (Mountain View, CA) Iris workstation.

Actin Purification, Polymerization/Depolymerization Assay, and Electron Microscopy

Actin was prepared from the acetone powder of rabbit back muscle, according to the method of Spudich and Watt [44]. For centrifugal assay, various concentrations of drug in 1 μl of DMSO were added to 99 μl of G-actin (0.2 mg/ml) in a solution consisting of 0.1 M KCl, 20 mM sodium phosphate buffer, pH 7.2, 1 mM $MgCl_2$, and 0.5 mM ATP (polymerizing buffer). After 30 min at room temperature, the reaction mixtures were centrifuged at 20,000 × g for 20 min (low speed) or at 100,000 × g for 1 hr (high speed). Precipitates and supernatants were analyzed by SDS-PAGE.

The effect of AmpH on actin polymerization was examined by fluorescence spectroscopy. Pyrene-labeled and unlabeled actin monomers were mixed in a solution of 5 mM Tris-HCl, pH 8.0, and 0.3 mM ATP to obtain a stock solution of 5% pyrene-actin. Polymerization was started by mixing of the actin stock solution with an appropriate salt solution in a plastic tube at 25°C. The mixture finally consisted of 0.1 M KCl, 20 mM sodium phosphate buffer, pH 7.2, 1 mM $MgCl_2$, 1 mM ATP, 1% DMSO, 0.2 mg/ml actin, and various concentrations of AmpH. The time course of polymerization of actin was monitored by a fluorescent spectroscope (excitation at 365 nm and emission at 407 nm). For depolymerization assay, 2 mg/ml actin in the stock solution was, beforehand, polymerized by the addition of $MgCl_2$ to 2.0 mM. Depolymerization was started by 10× dilution with a solution consisting of 5 mM Tris-HCl, pH 8.0, 50 μM $MgCl_2$, and 125 μM EGTA in a fluorescent spectroscope at 25°C and 75 s after the drug was added to the depolymerizing solution.

For electron microscopy, the polymerization of actin with or without drug was carried out in the polymerizing buffer containing 1% DMSO. A drop of each sample was applied to a collodion-coated copper grid and negatively stained with 1% uranyl acetate. The grid was observed under an electron microscope.

IEF, 2D-PAGE, and Immunoblotting

AmpH-treated HT1080 cells were suspended in sample buffer consisting of 40 mM Tris, 8 M urea, 4% CHAPS, and 20 mM DTT, and applied onto 13 cm Immobiline IEF gel strips, pH 4–7 (Amersham Biosciences Corp., Piscataway, NJ) that had been preswelled according to the manufacturer's protocol. For IEF-PAGE, the gel strips were electrophoresed with Multiphor II. For 2D-PAGE, the gel strips were placed on the 12.5% gel. After separation, the proteins were separated by 2D-PAGE, followed by transfer onto PVDF membrane. The protein-transferred PVDF membranes were stained with SYPRO Ruby, and protein spots were detected with a Molecular Imager FX (excitation = 488 nm, detection = 640 nm; Bio-Rad Laboratories Hercules, CA), followed by immunoblotting analyses performed with rabbit anti-actin IgG (20–33; Sigma, St. Louis, MO) as previously described [45].

Determination of the Amphidinolide H Binding Site by Mass Spectrometry

A complex of amphidinolide H and actin was prepared by incubation of 4.2 μM actin with 100 μM AmpH in polymerizing buffer for 30 min at room temperature. The molecular weight of the actin incubated with or without AmpH was determined by a reflex MALDI-TOF mass spectrometer (Bruker Daltonics, Billerica, MA). Following reduction with dithiothreitol and alkylation with iodoacetic acid, the proteins were digested with trypsin at 37°C for 4 hr, and the molecular weights of the generated peptides were determined by an ultraflex MALDI-TOF/TOF mass spectrometer (Bruker Daltonics).

Yeast Manipulation

The *ACT1* shuffle strain (ATU410; *MATa trp1 leu2 his3 ura3 ade2 can1-100 Δyrs1::HIS3 Δyrr1::TRP1 Δpdr1::hisG Δpdr3::hisG Δact1::kanMX6 pRS316-ACT1*) was constructed by PCR-based methods [46] from MLC30 [47]. Unless otherwise stated, cells were grown on YPDA medium (1% yeast extract, 2% polypeptone, 2% glucose, 0.02% adenine) except for plasmid-carrying strains. For halo assays, an overnight culture of yeast was grown in YPDA medium. Cells (100 μl) were added to 10 ml of 0.8% agar (cooled to 42°C), and the cell suspension was poured onto the surface of a YPDA plate. 10 μl of LatA (3 μg/ml), AmpH (100 μM), or DMSO alone was pipetted onto the center of thin, sterile paper disks (6 mm diameter; Advantec MFS, Inc., Tokyo, Japan). The disks were then placed on top of the agar. The plate was inverted and left at 30°C for 24–48 hr, until halos were clearly visible.

Acknowledgments

We thank Prof. G. Marriott for the gift of GFP-β-actin expression vector, and Prof. T. Miyakawa for the gift of the *Δyrr1 Δpdr1 Δpdr3 Δyor1* quadruplex deletion mutant (MLC30). We thank Drs. H. Nakayama, N. Kanoh, Y. Nagumo, and K. Ishida for their useful input. This study was supported by Grants for Basic Research (Bioarchitect Project and Chemical Biology Project) from RIKEN, and a Grant-in-Aid from the Ministry of Education, Culture, Sports, Science, and Technology of Japan.

Received: May 11, 2004
Revised: June 29, 2004
Accepted: July 1, 2004
Published: September 17, 2004

References

1. Frame, M.C., and Brunton, V.G. (2002). Advances in Rho-dependent actin regulation and oncogenic transformation. Curr. Opin. Genet. Dev. *12*, 36–43.
2. Staff, C.A. (2001). An introduction to cell migration and invasion. Scand. J. Clin. Lab. Invest. *61*, 257–268.
3. Pienta, K.J., and Coffey, D.S. (1991). Cell motility as a chemotherapeutic target. Cancer Surv. *11*, 255–263.
4. MacLean-Fletcher, S., and Polard, T.D. (1980). Mechanism of action of cytochalasin B on actin. Cell *20*, 329–341.
5. Cooper, J.A. (1987). Effects of cytochalasin and phalloidin on actin. J. Cell Biol. *105*, 1473–1477.
6. Coue, M., Brenner, S.L., Spector, I., and Korn, E.D. (1987). Inhibition of actin polymerization by latrunculin A. FEBS Lett. *213*, 316–318.
7. Spector, I., Shochet, N.R., Kashman, Y., and Groweiss, A. (1983). Latrunculins: novel marine toxins that disrupt microfilament organization in cultured cells. Science *219*, 493–495.
8. Saito, S., Watabe, S., Ozaki, H., Fusetani, N., and Karaki, H. (1994). Mycalolide B, a novel actin depolymerizing agent. J. Biol. Chem. *269*, 29710–29714.
9. Fusetani, N., Yasumuro, K., Matsunaga, S., and Hashimoto, K. (1989). Mycalolides A-C, hybrid macrolides of ulapualides and halichondramide, from a sponge of the genus *Mycale*. Tetrahedron Lett. *30*, 2809–2812.
10. Bubb, M.R., Spector, I., Bershadsky, A.F., and Ken, E.D. (1995). Swinholide A is a microfilament disrupting marine toxin that stabilizes actin dimers and severs actin filaments. J. Biol. Chem. *270*, 3463–3466.
11. Carmeli, S., and Kashman, Y. (1985). Structure of swinholide A, a new macrolide from the marine sponge *Theonella swinhoei*. Tetrahedron Lett. *26*, 511–514.
12. Yamada, K., Ojika, M., Ishigaki, T., Yoshida, Y., Ekimoto, H., and Arakawa, M. (1993). Aplyronine A, a potent antitumor substance and the congeners aplyronines B and C isolated from the sea hare *Aplysia kurodai*. J. Am. Chem. Soc. *115*, 11020–11021.
13. Saito, S.-y., Watabe, S., Ozaki, H., Kigoshi, H., Yamada, K., Fusetani, N., and Karaki, H. (1996). Novel actin depolymerizing macrolide aplyronine A. J. Biochem. (Tokyo). *120*, 552–555.
14. Terry, D.R., Spector, I., Higa, T., and Bubb, M.R. (1997). Misakinolide A is a marine macrolide that caps but does not sever filamentous actin. J. Biol. Chem. *272*, 7841–7845.
15. Kato, Y., Fusetani, N., Matsunaga, S., Hashimoto, K., Sakai, R., Higa, T., and Kashman, Y. (1987). Anititumor macrolides isolated from a marine sponge Theonella sp.: Structure revision of misakinolide A. Tetrahedron Lett. *49*, 6225–6228.
16. Wulf, E., Deboben, A., Bautz, F.A., Faulstich, H., and Wieland, T. (1979). Fluorescent phallotoxin, a tool for the visualization of cellular actin. Proc. Natl. Acad. Sci. USA *76*, 4498–4502.

17. Lengsfeld, A.M., Low, I., Wieland, T., Dancker, P., and Hasselbach, W. (1974). Interaction of phalloidin with actin. Proc. Natl. Acad. Sci. USA *71*, 2803–2807.
18. Bubb, M.R., Senderowicz, A.M.J., Sausville, E.A., Duncan, K.L.K., and Korn, E.D. (1994). Jasplakinolide, a cytotoxic natural product, induces actin polymerization and competitively inhibits the binding of phalloidin to F-actin. J. Biol. Chem. *269*, 14869–14871.
19. Bubb, M.R., Spector, I., Beyer, B.B., and Fosen, K.M. (2000). Effects of jasplakinolide on the kinetics of actin polymerization. J. Biol. Chem. *275*, 5163–5170.
20. Luesch, H., Yoshida, W.Y., Moore, R.E., Paul, V.J., and Mooberry, S.L. (2000). Isolation, structure determination, and biological activity of lyngbyabellin A from the marine cyanobacterium *Lyngbya majuscula*. J. Nat. Prod. *63*, 611–615.
21. Bai, R., Verdier-Pinard, P., Gangwar, S., Stessman, C.C., Mcclure, K.J., Sausville, E.A., Pettit, G.R., Bates, R.B., and Hamel, E. (2001). Dolastatin *11*, a marine depsipeptide, arrests cells at cytokinesis and induces hyperpolymerization of purified actin. Mol. Pharmacol. *59*, 462–469.
22. Marquez, B.L., Watts, K.S., Yokochi, A., Roberts, M.A., Verdier-Pinard, P., Jimenez, J.I., Hamel, E., Scheuer, P.J., and Gerwick, W.H. (2002). Structure and absolute stereochemistry of Hectochlorin, a potent stimulator of actin assembly. J. Nat. Prod. *65*, 866–871.
23. Bai, R., Covell, D.G., Liu, C., Ghosh, A.K., and Hamel, E. (2002). (-)-Doliculide, a new macrocyclic depsipeptide enhancer of actin assembly. J. Biol. Chem. *277*, 32165–32171.
24. Morton, W.M., Ayscough, K.R., and McLaughlin, P.J. (2000). Latrunculin alters the actin-monomer subunit interface to prevent polymerization. Nat. Cell Biol. *2*, 376–378.
25. Klenchin, V.A., Allingham, J.S., King, R., Tanaka, J., Marriott, G., and Rayment, I. (2003). Trisoxazole macrolide toxins mimic the binding of actin-capping proteins to actin. Nat. Cell Biol. *10*, 1058–1063.
26. Tanaka, J., Yan, Y., Choi, J., Bai, J., Klenchin, V.A., Rayment, I., and Marriott, G. (2003). Biomolecular mimicry in the actin cytoskeleton: mechanisms underlying the cytotoxicity of kabiramide C and related macrolides. Proc. Natl. Acad. Sci. USA *100*, 13851–13856.
27. Oda, T., Crane, Z.D., Dicus, C.W., Sufi, B.A., and Bates, R.B. (2003). Dolastatin 11 connects two long-pitch strands in F-actin to stabilize microfilaments. J. Mol. Biol. *328*, 319–324.
28. Kobayashi, J., Kubota, T., Endo, E., and Tsuda, M. (2001). Amphidinolides T2, T3, and T4, new 19-membered macrolides from the dinoflagellate Amphidinium sp., and the biosynthesis of amphidinolide T1. J. Org. Chem. *66*, 134–142.
29. Kobayashi, J., Shigemori, H., Ishibashi, M., Yamasu, T., Hirota, H., and Sasaki, T. (1991). Amphidinolides G and H: new potent cytotoxic macrolides from the cultured symbiotic dinoflagellate *Amphidinium* sp. J. Org. Chem. *56*, 5221–5224.
30. Kobayashi, J., Shimbo, K., Sato, M., Shiro, M., and Tsuda, M. (2000). Absolute stereochemistry of amphidinolides G and H. Org. Lett. *2*, 2805–2807.
31. Kobayashi, J., Shimbo, K., Sato, M., and Tsuda, M. (2002). Amphidinolides H2–H5, G2, and G3, new cytotoxic 2- and 27-membered macrolides from Dinoflagellate *Amphidinium* sp. J. Org. Chem. *67*, 6585–6592.
32. Hoehn, H., Sprague, C.A., and Martin, G.M. (1973). Effects of cytochalasin B on cultivated human diploid fibroblasts and its use for the isolation of tetraploid clones. Exp. Cell Res. *76*, 170–174.
33. Kijima, M., Yoshida, M., Sugita, K., Horinouchi, S., and Beppu, T. (1993). Trapoxin, an antitumor cyclic tetrapeptide, is an irreversible inhibitor of mammalian histone deacetylase. J. Biol. Chem. *268*, 22429–22435.
34. Taunton, J., Hassig, C.A., and Schreiber, S.L. (1996). A mammalian histone deacethylase related to the yeast transcriptional regulator Rpd3p. Science *272*, 408–411.
35. Griffith, E.C., Su, Z., Turk, B.E., Chen, S., Chang, Y.H., Wu, Z., Biemann, K., and Liu, J.O. (1997). Methionine aminopeptidase (type 2) is the common target for angiogenesis inhibitors AGM-1470 and ovalicin. Chem. Biol. *4*, 461–471.
36. Child, C.J., and Shoolingin-Jordan, P.M. (1998). Inactivation of the polyketide synthase, 6-methylsalicylic acid synthase, by the specific modification of Cys-204 of the β-ketoacyl synthase by the fungal mycotoxin cerulenin. Biochem. J. *330*, 933–937.
37. Ayscough, K.R., Stryker, J., Pokala, N., Sanders, M., Crews, P., and Drubin, D.G. (1997). High rates of actin filament turnover in budding yeast and roles for actin in establishment and maintenance of cell polarity revealed using the actin inhibitor latrunculin-A. J. Cell Biol. *137*, 399–416.
38. Lee, E., Shelden, E.A., and Knecht, D.A. (1998). Formation of F-actin aggregates in cells treated with actin stabilizing drugs. Cell Motil. Cytoskeleton *39*, 122–133.
39. Patterson, R.L., van Rossum, D.B., and Gill, D.L. (1999). Store-operated Ca^{2+} entry: evidence for a secretion-like coupling model. Cell *98*, 487–499.
40. Estes, J.E., Selden, L.A., and Gershman, L.C. (1981). Mechanism of action of phalloidin on the polymerization of muscle actin. Biochemistry *20*, 708–712.
41. Gettemans, J., Ville, Y.D., Vandekerckhove, J., and Waelkens, E. (1992). *Physarum* actin is phosphorylated as the actin-fragmin complex at residues Thr203 and Thr202 by a specific 80 kDa kinase. EMBO J. *11*, 3185–3191.
42. Tirion, M.M., ben-Avraham, D., Lorenz, M., and Holmes, K.C. (1995). Normal modes as refinement parameters for the F-actin model. Biophys. J. *68*, 5–12.
43. Usui, T., Kondoh, M., Cui, C.B., Mayumi, T., and Osada, H. (1998). Tryprostatin A, a specific and novel inhibitor of microtubule assembly. Biochem. J. *333*, 543–548.
44. Spudich, J.A., and Watt, S. (1971). The regulation of rabbit skeletal muscle contraction. I. Biochemical studies of the interaction of the tropomyosin-troponin complex with actin and the proteolytic fragments of myosin. J. Biol. Chem. *246*, 4866–4871.
45. Kondoh, M., Usui, T., Nishikiori, T., Mayumi, T., and Osada, H. (1999). Apoptosis induction via microtubule disassembly by an antitumour compound, pironetin. Biochem. J. *340*, 411–416.
46. Knop, M., Siegers, K., Pereira, G., Zachariae, W., Winsor, B., Nasmyth, K., and Schiebel, E. (1999). Epitope tagging of yeast genes using PCR-based strategy: more tags and improved practical routines. Yeast *15*, 963–972.
47. Miyamoto, Y., Machida, K., Mizunuma, M., Emoto, Y., Sato, N., Miyahara, K., Hirata, D., Usui, T., Takahashi, H., Osada, H., et al. (2002). Identification of *Saccharomyces cerevisiae* isoleucyl-tRNA synthetase as a target of the G1-specific inhibitor reveromycin A. J. Biol. Chem. *277*, 28810–28814.